BNL-223336-2022-TECH
C-A/AP/663

Transport of ~n0 Spin Vector in STAR and Polarimetry Regions RHIC Run 22 Optics

F. Méot

August 2022

Collider Accelerator Department
Brookhaven National Laboratory

U.S. Department of Energy
USDOE Office of Science (SC), Nuclear Physics (NP) (SC-26)

DISCLAIMER

Transport of $\vec{n}_0$ Spin Vector in STAR and Polarimetry Regions RHIC Run 22 Optics

François Méot & Vincent Schoefer

Tech. Note C-A/AP/663
BNL C-AD

Aug 23, 2022

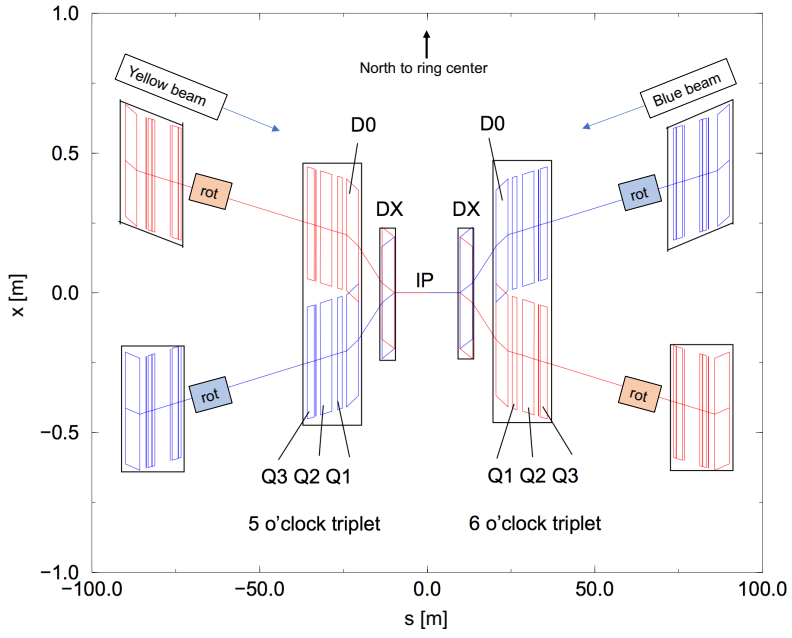

Contents

1 Introduction

Spin matrices are computed, and spin $\vec{n}_0$ vector is transported, from p-C polarimeter to H-Jet, and from Blue and Yellow upstream rotators to IP6.

Moving frame (O; X,Y,Z) in these simulations:

A direct triedra.
In both Blue and Yellow, longitudinal axis (X) is in beam direction, CW in Blue, CCW in Yellow, and Y axis points outward (curvature is negative, dispersion is positive). Vertical axis (Z) points up in BLUE (CW), down in YELLOW (CCW) (dipole field is positive and $// \vec{Z}$, in both cases).

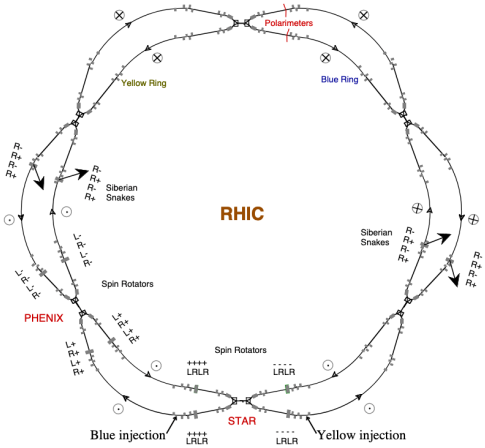

Figure 1: RHIC Blue and Yellow rings, snakes and rotators

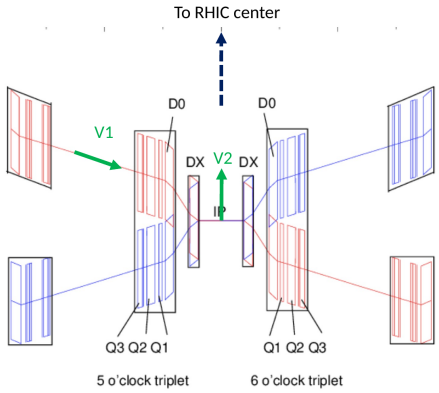

Figure 2: Typical spin $\vec{n}_0$ rotation in IR6 region, Yellow-CCW: a spin $\vec{V}_1 = (1, 0, 0)$ parallel to beam motion rotates (by $|G\gamma\alpha| \approx 100$ deg at 255 GeV, Sec. 2.2.1) to $\vec{V}_2 \approx (0, -1, 0)$ at IP6, under the effect of a field integral $BL = \alpha B\rho$ through DX and D0 dipoles.

In computing the spin transport matrices and spin $\vec{n}_0$ vector transport in Secs. 2.2 (Yellow) and 3.2 (Blue), two energies are considered, one is $E_{\rm tot} = 255.2$ GeV ($G\gamma = 487.6$) taken in the region of the usual polarized proton operation flat top, the other value considered is $E_{\rm tot} = 254.2$ GeV ($G\gamma = 485.75$), chosen as a new operation point early during Run 22 [1], in the aim of rotating the stable spin direction into the transverse plane, following the Blue snake incident [2, 3]. According to a numerical scan using snake field maps, rotators off [4] (computed in support to an actual experimental scan [5]), this new set point results in $\vec{n}_0$ just a couple of degrees away from its expected vertical orientation at IP6, Fig. 3.

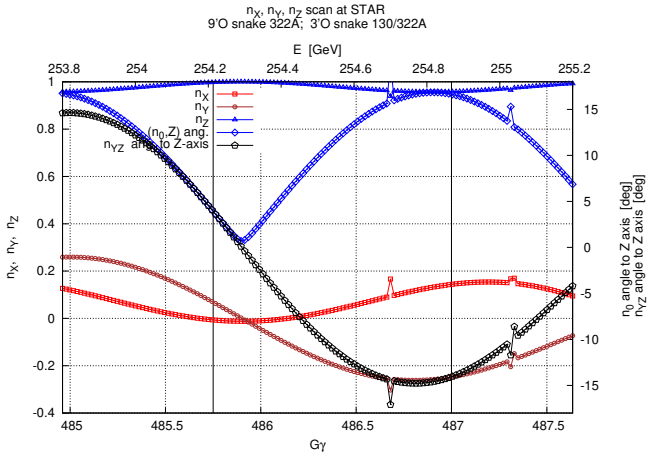

Figure 3: Spin scan versus energy: $\vec{n}_0$ components at STAR, and angle to Z axis (vertical). $\vec{n}_{\rm YZ}$ denotes the projection of $\vec{n}_0$ in the (Y,Z) plane [4].

2 Yellow

2.1 From p-C polarimeter to H-Jet

2.1.1 Injection energy ($G\gamma = 45.5$)

Run 22 injection optics is considered here. Reference orbits and optics for matrix calculations are displayed in Figs. 4 and 5.
Working hypotheses for these matrix computations are defined in App. A.

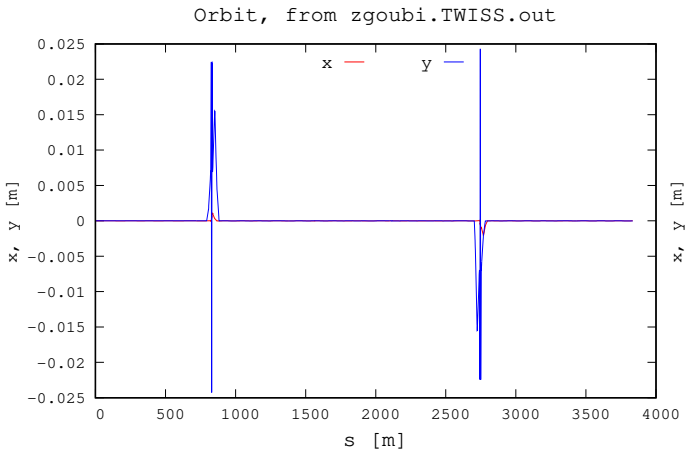

Figure 4: Yellow ring orbits in these spin matrix computations, including 8 snake field maps. .

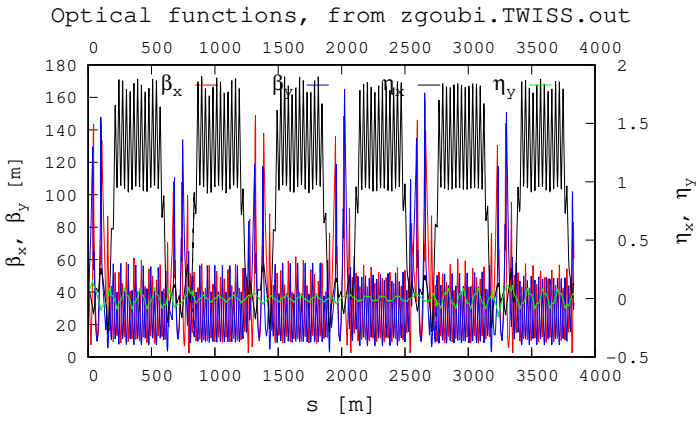

Figure 5: Yellow ring optics in these spin matrix computations.

The input file and gnuplot scritps for Figs. 6 and 7 simulation are available at

https : //sourceforge.net/p/zgoubi/code/HEAD/tree/trunk/exemples/RHIC/spin_RHICRun22/spinTransport_pCPol2Jet_YellowCCW_injection/

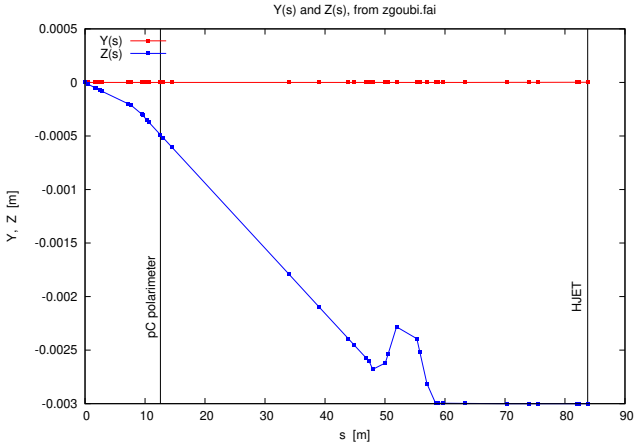

Figure 6: Yellow, CCW, $G\gamma = 45.5$. Orbit from entrance of YO12_TV5 (at s=0 in this graph) to H-JET: from a regular y=0 at YO12_TV5 (s=0, here) the orbit is positioned at y=-3 mm at H-JET.

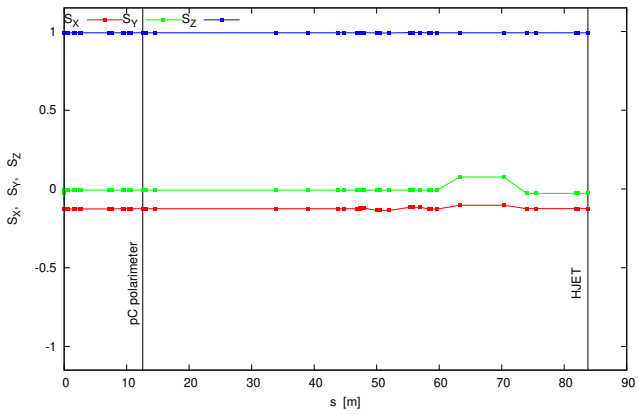

Figure 7: Yellow, CCW, $G\gamma = 45.5$. Spin components (X, Y, Z = long., radial, vertical), from YO12_TV5 (at s=0) to H-JET. A 9.4168353078 deg Z-rotation.

A fit is required (App. B) as initial spin $\vec{n}_0$ coordinates (at YO12_TV5, start of H-Jet orbit bump) are computed from spin coordinates at downstream p-C polarimeter location (polarization there known from measurements, see App. A). Coordinates at H-Jet, further downstream, are then obtained by transport over the p-C polarimeter to H-Jet section. The fitting includes the orbit separation bump at H-Jet. Orbit and spin coordinates in the region of concern are given in Figs. 6, 7.

Spin coordinates:

```
                          SX         SY         SZ
                          long.      radial     vert.
Entrance of YO12_TV5    -0.127813 -0.006996  0.991774          computed by fit
pC-pol                  -0.125    -0.007     0.992             measured
H-JET                   -0.124940 -0.027825  0.991774          transported from pC-pol.
```

Spin matrix, CCW, from p-C polarimeter to H-Jet:

```
       0.986520       -0.163616       -2.782134E-03
       0.163615        0.986524       -4.735205E-04
       2.822117E-03    1.193832E-05    0.999996

Trace =     2.9730482574;  spin precession acos((trace-1)/2) =     9.4168353078 deg
Precession axis :  ( 0.000070, 0.000034, 1.000000)
               ->  angle to (X,Y) plane, X axis, Z axis :   89.9955,   89.9960,    0.0045 deg
```

2.1.2 Store energy ($G\gamma = 485.75$)

Similar considerations as in Sec. 2.1.1, but for $G\gamma = 485.75$.
The input file and gnuplot scritps for this simulation are available at

https : //sourceforge.net/p/zgoubi/code/HEAD/tree/trunk/exemples/RHIC/spin_RHICRun22/spinTransport_pCPol2Jet_YellowCCW_store/

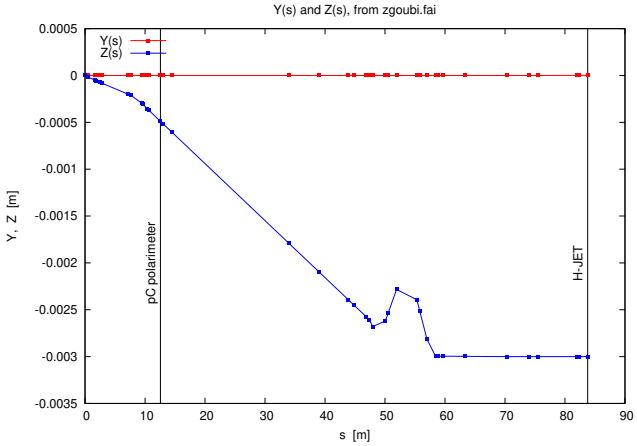

Figure 8: Yellow, CCW, $G\gamma = 485.75$. Orbit from entrance of YO12_TV5 (at s=0 in this graph) to H-JET: from a regular y=0 at YO12_TV5 (s=0, here) the orbit is positioned at y=-3 mm at H-JET.

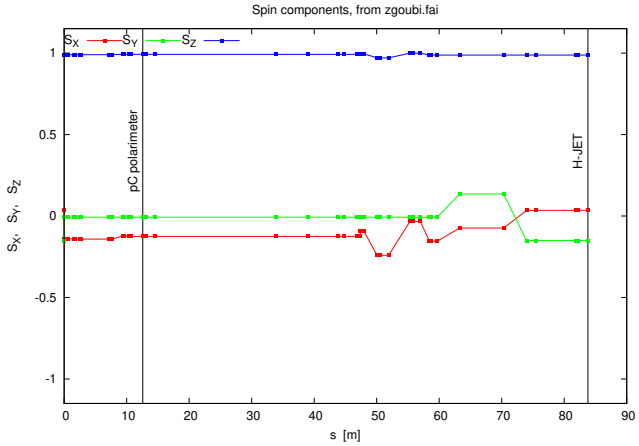

Figure 9: Yellow, CCW, $G\gamma = 485.75$. Spin components (X, Y, Z = long., radial, vertical), from YO12_TV5 (at s=0) to H-JET. A 100.5324516445 deg Z-rotation.

Spin coordinates:

```
                          SX         SY         SZ
                          long.      radial     vert.
Entrance of YO12_TV5    -0.154313 -0.007009  0.987997          computed by fit
pC-pol                  -0.125    -0.007     0.992             measured
H-JET                    0.035252 -0.150291  0.988013          transported from pC-pol.
```

Spin matrix, CCW, from p-C polarimeter to H-Jet:

```
      -0.182792       -0.983152        1.556594E-04
       0.983152       -0.182792        1.428139E-04
      -1.119543E-04    1.791421E-04     1.00000

Trace =     0.6344151999;  spin precession acos((trace-1)/2) =   100.5324516445 deg
Precession axis :  ( 0.000018, 0.000136, 1.000000)
               ->  angle to (X,Y) plane, X axis, Z axis :   89.9921,   89.9989,    0.0079 deg
```

2.2 From YI6_B3 rotator to IP6, 255 GeV

Run 22 pp store optics is considered here. The region of concern is sketched in Fig. 2. Two different $G\gamma$ cases assessed: $G\gamma = 485.750486$ and $G\gamma = 487.6353592$.

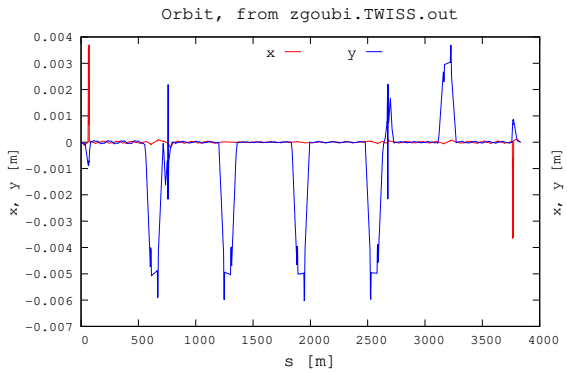

Figure 10: Yellow CCW ring orbits in these spin matrix computations.

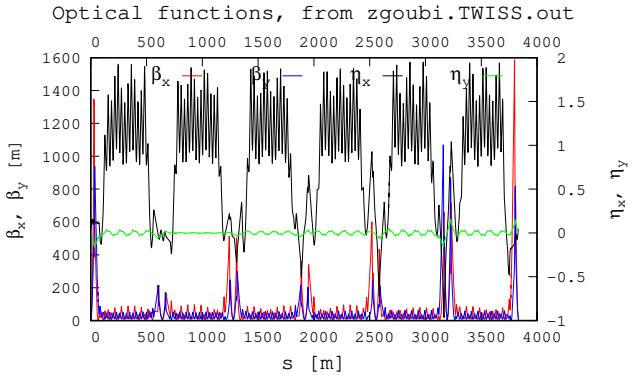

Figure 11: Yellow CCW ring optics with snake and rotator 16 field maps.

Reference Yellow ring orbits and optics for matrix calculations are displayed in Figs. 10 and 11. The YI6_B3 L+R+L+R+ rotator introduces a vertical orbit kick. This kick is locally compensated (a local orbit bump) using YI6_TV4 (located upstream of YI6 rotator) and YI6_TV2 (located between YI6 rotator and IP6).

Note that the necessary changes between the two different $G\gamma$ values concerned here, regarding (i) rotator coil currents to satisfy $\vec{n}_0$ alignment, and (ii) orbit kicker settings to close the local orbit bump at the rotator, are marginal (few per mil range).

2.2.1 $G\gamma = 485.750486$ $(E = 254.213\,\mathrm{GeV})$

The orbit bump is displayed in Fig. 12; note that the vertical separation bump has been cancelled for this computation. The components of a spin launched vertical ($n_{0,Z} > 0$, arbitrarily) at entrance of YI6_TV4 are propagated to IP6 in Fig. 13.

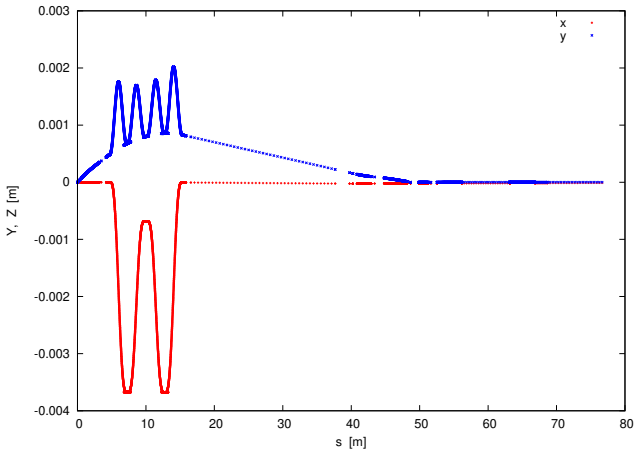

Figure 12: Yellow, CCW. Orbit from YI6_TV4 to IP6 (at the right), reference optical axis in these spin matrix computations.

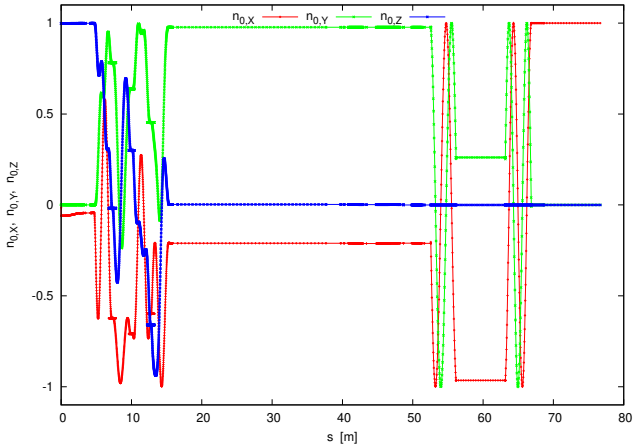

Figure 13: Yellow, CCW. Components of $\vec{n}_0$ vector in Serret-Frénet frame (X, Y, Z = long., radial, vertical), from vertical $\vec{n}_0$ at YI6_B3 rotator entrance (at s=0 in this graph) to longitudinal at IP6 (s≈77 m). Short back-forth segments in the $s \sim 5 - 15$ meter region are helix field maps artifacts. Rotator coil currents: $I_{\mathrm{out}} = 263.86963$ A $I_{\mathrm{in}} = 211.63029$ A

• L+R+L+R+ rotator spin matrix (13.11 m length):

```
                Spin transfer matrix, momentum group # 1 :

         -0.935387        0.247693       -0.252386
         -0.247646        5.064771E-02    0.967526
          0.252432        0.967514        1.396505E-02

   Trace =    -0.8707744836;  spin precession acos((trace-1)/2) =   159.2907968508 deg
   Precession axis :  (-0.000017,-0.713776,-0.700374) ->  angle to (X,Y) plane, X axis, Z axis :  -44.4570,   90.0010,  134.4570 deg

Sample spin, from vertical to mid-plane:
                 INITIAL                                          FINAL
          SX        SY        SZ        |S|         SX        SY        SZ        |S|       GAMMA   |Si,Sf|   (Z,Sf_yz) (Z,Sf)
 o  1  0.000000  0.000000  1.000000  1.000000    -0.252386  0.967526  0.013965  1.000000    270.9380   89.200    89.173    89.200    4
```

• Spin matrix from downstream end of rotator to IP6. The reference optical axis for that matrix is the orbit displayed in Fig. 12:

```
                Spin transfer matrix, momentum group # 1 :

         -0.211441        0.977390        1.029013E-03
         -0.977378       -0.211443        4.823990E-03
          4.932498E-03    1.425239E-05    0.999988

     Trace =     0.5771040767;  spin precession acos((trace-1)/2) =   102.2072199997 deg
     Precession axis :  (-0.0024605, -0.0019969, -0.9999950)  ->  angle to (X,Y) plane, to X axis :   -89.8184,    90.1410 deg

Sample spin, 102 deg Z-precession to long. through D0 \& DX:
                 INITIAL                                          FINAL
          SX        SY        SZ        |S|         SX        SY        SZ        |S|       GAMMA   |Si,Sf|   (Z,Sf_yz) (Z,Sf)
 o  1 -0.197788  0.980242 -0.002266  1.000000     0.999897 -0.013963 -0.003228  1.000000    270.9380 -102.207   102.692    90.185    4
```

2.2.2 $G\gamma = 487.6353592 \quad (E = 255.20\,\mathrm{GeV})$

Compared to the previous $G\gamma$ value, the orbit bump (Fig. 12) is essentially unchanged (quadrupoles have the same strengths, rotator setting changes marginally). The components of a spin launched vertical at entrance of YI6_TV4 are propagated to IP6 in Fig. 14

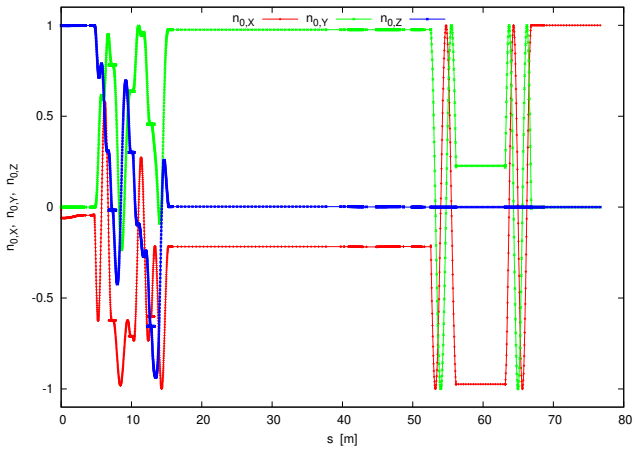

Figure 14: Yellow, CCW. Spin components (X, Y, Z = long., radial, vertical), from YI6_B3 rotator (entrance at s=3760) to IP6. Back-forth segments in the 5-15 meter region are field map artifacts Rotator coil currents: $I_{\mathrm{out}} = 263.65812\,\mathrm{A}$ $I_{\mathrm{in}} = 211.07041\,\mathrm{A}$

• L+R+L+R+ rotator spin matrix (13.11 m length):

```
                Spin transfer matrix, momentum group # 1 :

         -0.931964        0.253759       -0.258939
         -0.253713        5.370981E-02    0.965787
          0.258985        0.965775        1.432637E-02

   Trace =    -0.8639276321;  spin precession acos((trace-1)/2) =   158.7430369654 deg
   Precession axis :  (-0.000017,-0.714278,-0.699862) ->  angle to (X,Y) plane, X axis, Z axis :  -44.4160,   90.0010,  134.4160 deg

Sample spin, from vertical to mid-plane:
                 INITIAL                                          FINAL
          SX        SY        SZ        |S|         SX        SY        SZ        |S|       GAMMA   |Si,Sf|   (Z,Sf_yz) (Z,Sf)
 o  1  0.000000  0.000000  1.000000  1.000000    -0.258939  0.965787  0.014326  1.000000    271.9893   89.179    89.150    89.179    4
```

• Spin matrix from downstream end of rotator to IP6. The reference optical axis for that matrix is the orbit displayed in Fig. 12:

```
                Spin transfer matrix, momentum group # 1 :

         -0.217306        0.976099        2.862886E-03
         -0.976015       -0.217325        1.286390E-02
          1.317862E-02    1.181332E-06    0.999913

   Trace =     0.5652827908;  spin precession acos((trace-1)/2) =   102.5539383428 deg
   Precession axis :  (-0.006589,-0.005284,-0.999964) ->  angle to (X,Y) plane, X axis, Z axis :  -89.5161,   90.3775,  179.5161 deg

Sample spin, 102 deg Z-precession to long. through D0 \& DX:
                 INITIAL                                          FINAL
          SX        SY        SZ        |S|         SX        SY        SZ        |S|       GAMMA   |Si,Sf|   (Z,Sf_yz) (Z,Sf)
 o  1 -0.197786  0.980243 -0.002268  1.000000     0.999777 -0.020885 -0.003274  1.000000    271.9893 -102.604    98.803    90.188    4
```

3 Blue

3.1 From p-C polarimeter to H-Jet

3.1.1 Injection energy ($G\gamma = 45.5$)

Run 22 injection optics is considered here. Reference orbits and optics for matrix calculations are displayed in Figs. 15 and 16.
Working hypotheses for these matrix computations are defined in App. A.

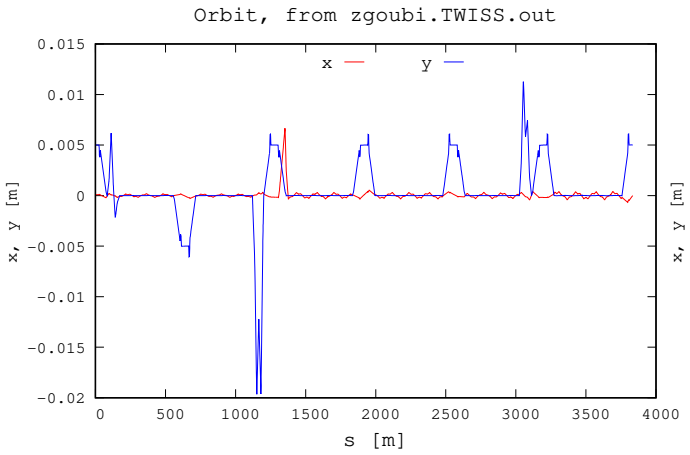

Figure 15: Blue ring orbits in these spin matrix computations, including helical snake dipole fields.

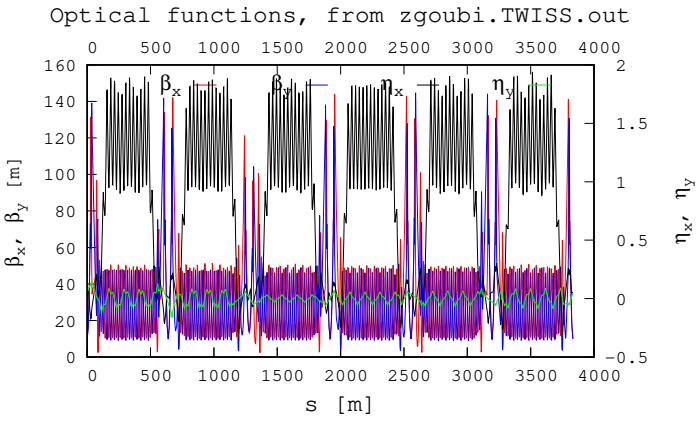

Figure 16: Blue ring optics in these spin matrix computations.

The input file and gnuplot scritps for Figs. 17 and 18 simulation are available at

https : //sourceforge.net/p/zgoubi/code/HEAD/tree/trunk/exemples/RHIC/spin_RHICRun22/spinTransport_pCPol2Jet_Blue_injection/

A fit is required (App. C) as H-Jet, where $\vec{n}_0$ coordinates are to be determined, is at the beginning of the optical sequence, whereas p-C polarimeter, where polarization is known, is near the downstream end. The fitting includes the orbit separation bump at H-Jet. Orbit and spin coordinates in the region of concern are given in Figs. 17, 18.

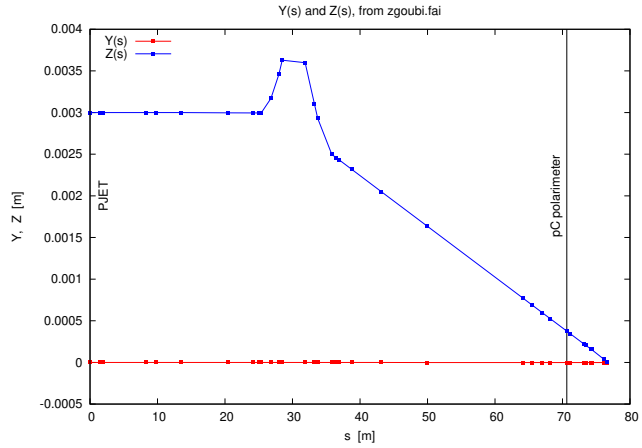

Figure 17: Blue, CW, $G\gamma = 45.5$. Orbit from H-Jet (at s=0) to exit of BI12_TV4

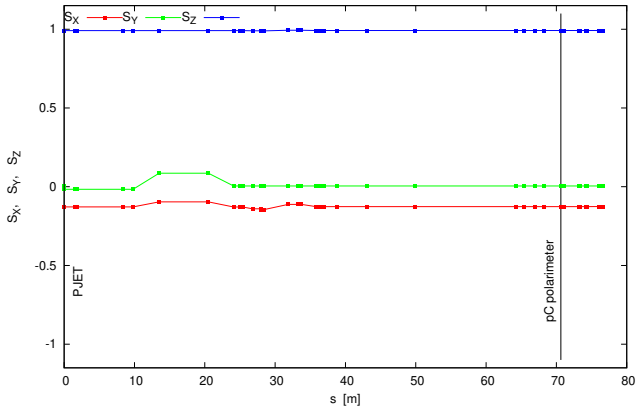

Figure 18: Blue, CW, $G\gamma = 45.5$. Spin components (X, Y, Z = long., radial, vertical), from H-Jet (at s=0) to exit of BI12_TV4 A 9.5462547133deg Z-rotation.

Spin coordinates:

```
                          SX         SY         SZ
                          long.      radial     vert.
H-JET                  -0.130761 -0.016932  0.991269           deduced
pC-pol                 -0.128953  0.004998  0.991638           measured
Exit of BI12_TV4       -0.131762  0.005000  0.991269           transported from pC-pol.
```

Spin matrix, CW, from H-Jet to p-C polarimeter:

```
                  Spin transfer matrix, momentum group # 1 :

       0.986152         0.165844       -4.285021E-06
      -0.165844         0.986152        1.189786E-05
       6.198867E-06    -1.102245E-05     1.00000

 Trace =     2.9723040754;  spin precession acos((trace-1)/2) =     9.5462547133 deg
 Precession axis :  (-0.000069,-0.000032,-1.000000)
                ->  angle to (X,Y) plane, X axis, Z axis :  -89.9956,   90.0040,  179.9956 deg
```

3.1.2 Store energy ($G\gamma = 485.75$)

Similar considerations as in Sec. 3.1.1, but for $G\gamma = 485.75$.
The input file and gnuplot scritps for this simulation are available at

https : //sourceforge.net/p/zgoubi/code/HEAD/tree/trunk/exemples/RHIC/spin_RHICRun22/spinTransport_pCPol2Jet_Blue_store/

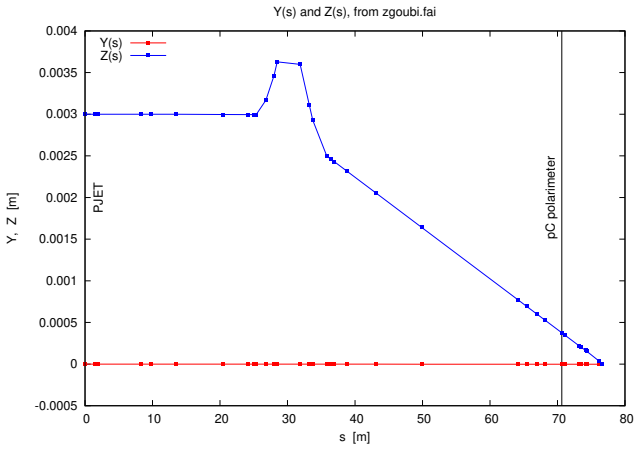

Figure 19: Blue, $G\gamma = 485.75$. Orbit from H-Jet (at s=0) to exit of BI12_TV4

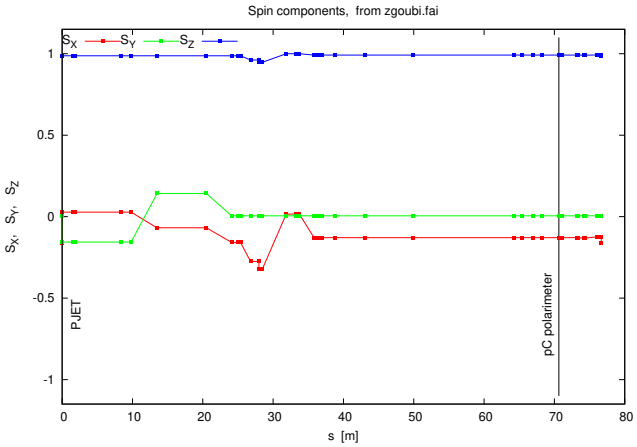

Figure 20: Blue, $G\gamma = 485.75$. Spin components (X, Y, Z = long., radial, vertical), from H-Jet (at s=0) to exit of BI12_TV4 A 101.91399277 deg Z-rotation.

Spin coordinates:

```
                          SX         SY         SZ
                          long.      radial     vert.
H-JET                   0.027924 -0.155789  0.987396           deduced
pC-pol                 -0.128953  0.004998  0.991638           measured
Exit of BI12_TV4       -0.158304  0.005013  0.987378           transported from pC-pol.
```

Spin matrix, CW, from H-Jet to p-C polarimeter:

```
                  Spin transfer matrix, momentum group # 1 :

      -0.206443         0.978459       -1.077103E-04
      -0.978459        -0.206443        1.761542E-04
       1.501235E-04     1.417559E-04     1.00000

 Trace =     0.5871136987;  spin precession acos((trace-1)/2) =   101.9139927706 deg
 Precession axis :  (-0.000018,-0.000132,-1.000000)
                ->  angle to (X,Y) plane, X axis, Z axis :  -89.9924,   90.0010,  179.9924 deg
```

3.2 From BI5_B3 rotator to IP6, 255 GeV

Run 22 pp store optics is considered here. The region of concern is sketched in Fig. 2. Two different $G\gamma$ cases assessed: $G\gamma = 485.750486$ and $G\gamma = 487.6353592$.

The BI5 R-L-R-L- rotator introduces a vertical orbit kick. This kick is locally compensated (a local orbit bump) using BI5_TV4 (located a little upstream of BI5 rotator) and BI5_TV2 (located between BI5 rotator and IP6).

Note that the necessary changes between the two different $G\gamma$ values concerned here, regarding (i) rotator coil currents to satisfy $\vec{n}_0$ alignment, and (ii) orbit kicker settings to close the local orbit bump at the rotator, are marginal (few per mil range).

3.2.1 $G\gamma = 485.750486$

The orbit bump is displayed in Fig. 21; note that the IP6 vertical separation bump seen in Fig. 15 has been cancelled for the present computation.

The components of a spin launched vertical at entrance of BI5_TV4 are propagated to IP6 in Fig. 22.

Note the following: removing the local vertical orbit compensation (thus the reference axis for the sin matrix computation wanders unclosed) changes only marginally the BI5 to IP6 spin matrix - due to the marginal vertical excursion anyway, a fraction of a mm.

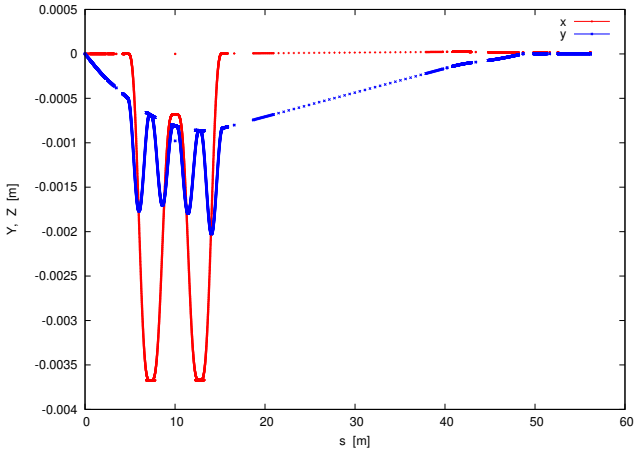

Figure 21: Blue, CW. Reference orbit in this matrix computation, from BI5_B3 rotator to IP6. The origin s=0 is at BI5_TV4; the rotator extends over $3.46 \leq s \leq 16.57\,\mathrm{m}$ - back-forth segments in that region are field map artifacts.

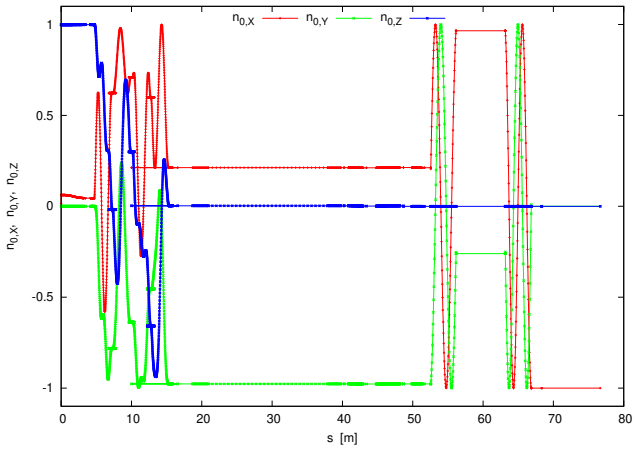

Figure 22: Blue, CW. Spin components (X, Y, Z = long., radial, vertical), from BI5_B3 rotator (in s∼5-15 m region) to IP6. Short back-forth segments in the 5-15 meter region are field map artifacts. Rotator coil currents: $I_{\mathrm{out}} = 263.63306\,\mathrm{A}$ $I_{\mathrm{in}} = 210.82667\,\mathrm{A}$

• R-L-R-L- rotator spin matrix (13.11 m rotator section extending over $3.46254 \leq s \leq 16.571\,\mathrm{m}$ - note that end drifts do not change the matrix):

```
                Spin transfer matrix, momentum group # 1 :

        -0.930628        0.256159        0.261370
        -0.255999        5.471565E-02   -0.965127
        -0.261527       -0.965085        1.465655E-02

   Trace =    -0.8612555821;  spin precession acos((trace-1)/2) =   158.5328885061 deg
   Precession axis :  ( 0.000058, 0.714405,-0.699732) ->  angle to (X,Y) plane, X axis, Z axis :  -44.4055,   89.9967,  134.4055 deg


Sample spin, from vertical to mid-plane:
           SX        SY        SZ        |S|         SX        SY        SZ        |S|       GAMMA   |Si,Sf|   (Z,Sf_yz) (Z,Sf)
 o  1  0.000000  0.000000  1.000000  1.000000     0.261370 -0.965127  0.014657  1.000000    270.9380   89.160   89.130   89.160    4
```

• Spin matrix from downstream end of rotator (at s=16.571300 m in Fig. 21) to IP6. The reference optical axis for that matrix is the orbit displayed in Fig. 21:

```
                Spin transfer matrix, momentum group # 1 :

        -0.213004        0.977047       -2.838870E-03
        -0.976960       -0.213023       -1.301559E-02
        -1.332159E-02    1.090214E-06    0.999911

   Trace =     0.5738841394;  spin precession acos((trace-1)/2) =   102.3016152391 deg
   Precession axis :  ( 0.006661, 0.005365,-0.999963) ->  angle to (X,Y) plane, X axis, Z axis :  -89.5100,   89.6183,  179.5100 deg


Sample spin, 102 deg Z-precession to long. through D0 \& DX:
          SX        SY        SZ        |S|         SX        SY        SZ        |S|       GAMMA   |Si,Sf|   (Z,Sf_yz) (Z,Sf)
 o  1  0.213002 -0.977048  0.002838  1.000000    -1.000000  0.000002 -0.000001  1.000000    270.9380 -102.298  109.371   90.000    4
```

3.2.2 $G\gamma = 487.6353592$

Compared to the previous $G\gamma$ value, the orbit bump is essentially unchanged (quadrupoles have the same strengths, rotator setting changes marginally). The reference orbit is essentially as in Fig. 21. The components of a spin launched vertical ($n_{0,Z} > 0$, arbitrarily) at entrance of BI5_TV4 are propagated to IP6 in Fig. 23.

Note the following: removing the local vertical orbit compensation (thus the reference axis for the sin matrix computation wanders unclosed) changes only marginally the BI5 to IP6 spin matrix - due to the marginal vertical excursion anyway, a fraction of a mm.

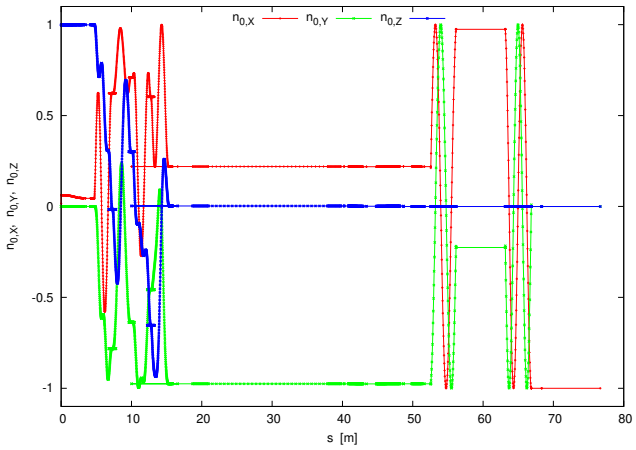

Figure 23: Blue, CW. Spin components (X, Y, Z = long., radial, vertical), from BI5_B3 rotator (in s∼5-15 m region) to IP6. Back-forth segments in the 5-15 meter region are field map artifacts. Rotator coil currents: $I_{\rm out} = 263.84575\,\mathrm{A}$ $I_{\rm in} = 211.38635\,\mathrm{A}$

• R-L-R-L- rotator spin matrix (13.11 m rotator section extending over $3.46254 \le s \le 16.571$ m - note that end drifts do not change the matrix):

```
                Spin transfer matrix, momentum group # 1 :

        -0.930628        0.256159        0.261370
        -0.255999        5.471693E-02   -0.965127
        -0.261527       -0.965085        1.465511E-02

   Trace =    -0.8612559177;  spin precession acos((trace-1)/2) =   158.5329147732 deg
   Precession axis :  ( 0.000058, 0.714406,-0.699732) ->  angle to (X,Y) plane, X axis, Z axis :  -44.4055,   89.9967,  134.4055 deg


Sample spin, from vertical to mid-plane:
                INITIAL                                         FINAL
           SX        SY        SZ        |S|         SX        SY        SZ        |S|       GAMMA   |Si,Sf|   (Z,Sf_yz) (Z,Sf)
 o  1  0.000000  0.000000  1.000000  1.000000     0.261370 -0.965127  0.014655  1.000000    271.9893   89.160   89.130   89.160    4
```

• Spin matrix from downstream end of rotator (at s=16.571300 m) to IP6. The reference optical axis for that matrix is the orbit displayed in Fig. 21:

```
                Spin transfer matrix, momentum group # 1 :

        -0.219764        0.975549       -2.925070E-03
        -0.975462       -0.219784       -1.297848E-02
        -1.330402E-02    1.086702E-06    0.999911

   Trace =     0.5603631397;  spin precession acos((trace-1)/2) =   102.6983687515 deg
   Precession axis :  ( 0.006652, 0.005320,-0.999964) ->  angle to (X,Y) plane, X axis, Z axis :  -89.5120,   89.6188,  179.5120 deg


Sample spin, 102 deg Z-precession to long. through D0 \& DX:
                INITIAL                                         FINAL
           SX        SY        SZ        |S|         SX        SY        SZ        |S|       GAMMA   |Si,Sf|   (Z,Sf_yz) (Z,Sf)
 o  1  0.261370 -0.965127  0.014655  1.000000    -0.999011 -0.043027  0.011175  1.000000    271.9893 -102.675   75.889   89.360    4
```

Appendix

A Working hypotheses

- Made measurements of the spin direction at the pC polarimeter.
- Track those spin coordinates from pC to the Jet.
- Below are the measured spin vectors together with the statistical errors. Here (x,y,z) is horizontal, vertical, longitudinal.

- The convention for horizontal is from the polarimeter people:
BLUE +X = radially OUTWARD from ring center
YELLOW +X = radially INWARD from ring center
+Longitudinal is beam direction, +vertical is up.

Design vertical orbit excursion (to position the beams at the Jet the way they want), corrector strengths in the region are as follows (in mrad):

BLUE	angle (mrad)
bo11-tv5	-0.0101
bo11-tv3	-0.0224
bi12-tv2	-0.0372
bi12-tv4	-0.0255

YELLOW	angle (mrad)
yi11-tv4	-0.0763
yi11-tv2	-0.1098
yo12-tv3	-0.0672
yo12-tv5	-0.0303

Polarization:

BLUE

Sx0	err	Sy0	err	Sz0	err
0.005	0.009	0.992	0.01	-0.129	0.074

YELLOW

Sx0	err	Sy0	err	Sz0	err
-0.007	0.011	0.992	0.01	-0.125	0.078

B Input data file for a fit, Yellow-CCW

This file generates Figs. 6, 7.

```
pp22-yellow-CCW_pCpol2JET.INC.dat
'OBJET'
79.366778931425273 * 1d3
2
4 1
0.  0.   0.  0.    0.  1. 'o'
0.  0.   0.  0.    0.  1. 'o'
0.  0.   0.  0.    0.  1. 'o'
0.  0.   0.  0.    0.  1. 'o'
1 1 1 1
'PARTICUL'
PROTON
'SPNTRK'
4
1. 0. 0.
0. 1. 0.
0. 0. 1.
-0.127813 -0.006996 0.991774
'FAISTORE'
zgoubi.fai all
1

'INCLUDE'
1
SCALING.inc[scaling_S:scaling_E]

'INCLUDE'
1
pp22-yellow-CCW_JETBumpKickersON.INC.dat[YO12_QS5:G12_PJETX]

'FIT2'
5                                ! 5 variables:
3 40 0 [-1.1,1.1]                ! Initial 3 spin coordinates
3 41 0 [-1.1,1.1]
3 42 0 [-1.1,1.1]
6 44 0 [-1.e5,1.e5]              ! YO12_TV5
6 48 0 [-1.e5,1.e5]              ! YO12_TV3
7 1e-10                          ! 7 constraints:
10 4 4 8   1.        .01  0      ! Initial spin modulus.
10 4 1 27 -0.125016   1.  0      ! Three spin coordinates and spin modulus.
10 4 2 27 -0.007001   1.  0
10 4 3 27  0.992130   1.  0
10 4 4 27  1.        .01  0
3 1 4 #End -0.3       1.  0      ! Z at JET
3 1 5 #End  0.        .1  0      ! P at JET

'FAISCEAU'
'SPNPRT'   MATRIX

'SYSTEM'
2
gnuplot < ./gnuplot_Zfai_YZ-s.gnu
gnuplot < ./gnuplot_Zfai_s-SXYZ.gnu
'END'
```

Outcomes (from zgoubi.res):

```
         INITIAL  S_X, _Y, _Z                CURRENT  S_X, _Y, _Z

\vec n_0 at begining:
 o  1 -0.127813 -0.006996  0.991774  1.  -0.127813 -0.006996  0.991774 1.

\vec_n0 at p-C polarimeter:
 o  1 -0.127813 -0.006996  0.991774  1.  -0.125009 -0.006996  0.992131 1.

\vec_n0 at H-Jet:
 o  1 -0.127813 -0.006996  0.991774  1.  -0.124939 -0.027825  0.991774 1.
```

C Input data file for a fit, case of Blue

This file generates Figs. 17, 18.

```
pp22-blue_pCpol2JET.INC.dat
'OBJET'      1
79.366778931425273 * 1d3
2
4 1
0.  0.   0.3  0.    0.  1. 'o'
0.  0.   0.3  0.    0.  1. 'o'
0.  0.   0.3  0.    0.  1. 'o'
0.  0.   0.3  0.    0.  1. 'o'
1 1 1 1
'PARTICUL'   2
PROTON
'SPNTRK'     3
4
1. 0. 0.
0. 1. 0.
0. 0. 1.
-0.12799042  -1.64680845E-02 0.99163863
'FAISTORE'   5
zgoubi.fai all
1

'INCLUDE'
1
SCALING.inc[scaling_S:scaling_E]

'INCLUDE'
1                  ! CW beam line sequence from H-Jet to p-C polarimeter:
pp22-255GeV-e0_injection_TWISS.dat[G12_PJETX:BI12_QS4]

'FAISCEAU'
'SPNPRT'   MATRIX

'FIT2'
5                                ! 5 variables:
3 40 0 [-1.1,1.1]                ! Initial 3 spin coordinates - at H-Jet
3 41 0 [-1.1,1.1]
3 42 0 [-1.1,1.1]
6 36 0 [-1.e5,1.e5]              ! BI12_TV2 in SCALING
6 40 0 [-1.e5,1.e5]              ! BI12_TV4   "
7 1e-10                          ! 7 constraints:
10 4 4 8   1.    .01  0        ! Initial spin modulus.
10 4 1 58 -.129   1.  0        ! Three spin coordinates and spin modulus at pC-pol.
10 4 2 58  5E-03  1.  0
10 4 3 58  .992   1.  0
10 4 4 58  1.    .01  0
3  1 4 #End  .0  1.  0        ! Cancel H-Jet separation bump at BI12_TV4
3  1 5 #End  .0  .1  0

'SYSTEM'
2
gnuplot < ./gnuplot_Zfai_YZ-s.gnu
gnuplot < ./gnuplot_Zfai_s-SXYZ.gnu


'END'
```

Outcomes (from zgoubi.res):

```
         INITIAL  S_X, _Y, _Z                CURRENT  S_X, _Y, _Z

\vec_n0 at H-Jet:
 o  1 -0.130761 -0.016932  0.991269 1.  -0.130761 -0.016932  0.991269 1.

\vec_n0 at p-C polarimeter:
 o  1 -0.130761 -0.016932  0.991269 1.  -0.128953  0.004998  0.991638 1.

\vec_n0 at B12_TV4:
 o  1 -0.130761 -0.016932  0.991269 1.  -0.131762  0.005000  0.991269 1.
```

References

[1] V. Schoefer, RHIC Morning Status Meeting: 12/22/2021.

[2] V. Schoefer et als. RHIC Polarized Proton Operation in Run 22. WEPOPT031. Procs IPAC 2022 Conference, Bangkok. https://ipac2022.vrws.de/papers/wepost031.pdf

[3] F. Méot et als. RHIC Blue Snake Blues. WEPOPT019. Procs IPAC 2022 Conference, Bangkok. https://ipac2022.vrws.de/papers/wepopt019.pdf

[4] F. Méot et als., RHIC Run 22, 9 o'clock, a Snake in the Blue, BNL C-AD Tech Note C-A/AP/661 (June 2022).

[5] V. Schoefer, RHIC Morning Status Meeting: 12/23/2021. RHIC Morning Status Meeting: 12/30/2021.